Available online at www.sciencedirect.com

jmr&t Journal of Materials Research and Technology

www.jmrt.com.br

Original Article

Highly efficient photocatalytic performance of $Cu_2O@TiO_2$ nanocomposite: influence of various inorganic oxidants and inorganic anions

Wagih A. Sadik[a], *Abdel-Ghaffar M. El-Demerdash*[a], *Adel W. Nashed*[a], *Amr A. Mostafa*[a], *Hesham A. Hamad*[b,*]

[a] *Materials Science Department, Institute of Graduate Studies and Research (IGSR), Alexandria University, Alexandria, Egypt*
[b] *Fabrication Technology Department, Advanced Technology and New Materials Research Institute (ATNMRI), City of Scientific Research and Technological Applications (SRTA-City), New Borg El-Arab City, 21934, Alexandria, Egypt*

ARTICLE INFO

Article history:
Received 15 August 2019
Accepted 3 September 2019
Available online 26 September 2019

Keywords:
Photocatalytic oxidation
$Cu_2O@TiO_2$ nanocomposite
Inorganic oxidants
AR8 dye degradation
Electrical energy per order.

ABSTRACT

This work offers the facile synthesis of $Cu_2O@TiO_2$ nanocomposites by solid state reaction towards the elimination of Acid-Red 8 (AR8) dye as a target pollutant model through the photocatalytic oxidation system. Another goal is to assess the capacity of various inorganic oxidants that act as alternative electron acceptor for $Cu_2O@TiO_2$ mediated photocatalytic oxidation. The prepared nanocomposite was analyzed by various analysis instruments, and their photocatalytic performance was systemically assessed with respect to the removal of AR8 dye. Upon irradiation, compared to pure Cu_2O and pure TiO_2 alone, the $Cu_2O@TiO_2$ has exhibited a higher photocatalytic performance which show that the combining TiO_2 (n-type) with Cu_2O (p-type) has been improved the electron mobility and subsequently decreasing the rate of electron-hole recombination. A kinetic study is confirmed that the degradation of AR8 has been obeyed the pseudo-first-order model. The perfection of the photocatalytic activity is achieved by using various inorganic oxidants such as; H_2O_2, $Na_2S_2O_8$ and $NaIO_4$ so as to produce an electron scavenger. Also, the apparent rate constant (k_{app}) and apparent quantum yield (Q_{app}) are higher for all oxidants than without oxidants, while is lower in terms of electrical energy per order (E_{EO}) and half-life time ($t^{0.5}$). Periodate ion has considered the most efficient oxidant when compared with other oxidants for enhancing the photocatalytic activity via the formation of various reactive oxygen species. The degradation efficiency of these catalytic systems could be arranged in an ascending order: $Cu_2O@TiO_2/NaIO_4 > Cu_2O@TiO_2/Na_2S_2O_8 > Cu_2O@TiO_2/H_2O_2 > Cu_2O > TiO_2$.

1. Introduction

Recently, the shortage of water is becoming more severe problem due to an environmental pollution, rapid industrial growth, uncontrolled groundwater progress and reducing the water resources. Hence, the fixing of these problems and

* *Corresponding author.*
E-mail: heshamaterials@hotmail.com (H.A. Hamad).
https://doi.org/10.1016/j.jmrt.2019.09.007

cleaning of wastewater are urgently vital [1,2]. In the recent decades, there are enormous application of the dyes in many industries, especially in textile, chemical, pharmaceutical, food, and cosmetics industries which is the main involvement of the generation and growth of hazardous and toxic chemicals like amines and cyanides [3].

There is great battery in the removal of dye-containing wastewater by conventional methods like biological treatment [4], coagulation- flocculation [5], anodic oxidation [6], electrocoagulation [7], ozonation [8], reverse osmosis [9], and adsorption [10]. All of these techniques suffer from one or more limitation, and none of them is able to completely remove dyes from wastewater. The target of complete mineralization of organic toxic dyes is being established by advanced oxidation processes (AOPs) in order to respond to the progressive growth of the water pollution. Among them, heterogeneous photocatalysis is esteemed a motivating technique with today's challenging demands especially for clean water technology [11,12].

Nanostructured TiO_2 is considered as a well-known photocatalyst for the highly efficient performance for decomposition of textile pollutants in water [13]. The destruction of organic pollutants by titania in the presence of suitable light is as a result of production of hydroxyl radical, very strong oxidant, that are the key of using the photocatalyst for oxidation of organic molecules. Also, there were many efforts for improving the photocatalytic activity by combination with other oxidants [14]. Great challenges have been made in order to improve the performance of titania, mainly joint with other semiconductor, regardless the excellent prospect of efficient photocatalytic mineralization of toxic dyes in water [15].

Sensitization of n-type such as; TiO_2 with p-type such as; Cu_2O is an effective path for fabrication TiO_2 based photocatalyst with extended absorption and subsequently improved the photocatalytic activity. This is due to the low band gap of Cu_2O ($E_0 = 1.9–2.2$ eV) and the formation of heterostructure between TiO_2 and Cu_2O that helps the separation and transportation of the photo induced charge carriers in Cu_2O@TiO_2 heterojunction nanocomposite, and hence declines the opportunity of recombination and improves the photocatalytic properties [16]. Also, the synergistic effect between TiO_2 and Cu_2O is very important for improving the charge separation and leads to much higher photocatalytic activity than pure TiO_2 and Cu_2O [17,18].

Many research groups concerned with the fabrication of Cu_2O@TiO_2 in order to make a progress in the destruction of organic contaminants from water. The photocatalytic activity of TiO_2/zeolite (TZ) was improved the photocatalytic degradation of bisphenol A(BPA) by adding Cu_2O [19]. Mixed oxides of Cu_2O-TiO_2 was synthesized on a copper substrate for reduction of 2,2′,4,4′-tetrabromodiphenyl ether (BDE47) [20]. Also, the morphology is significant factor for enhancing the photocatalytic activity. The Cu_2O/TiO_2 heterostructure hollow spheres (Cu_2O/TiO_2 HS) for removal of Rhodamine B as a result of design the heterojunction between TiO_2 and Cu_2O [21]. The degradation of reactive blue 49 (RB 49) dye is observed by using 4 wt.% Cu_2O-CuO/TiO_2 catalyst [22].

To date, there is no studies concerning the various inorganic oxidants using Cu_2O@TiO_2 as a photocatalyst for destruction of toxic dyes in an aqueous solution. Herein, it is in those perspectives as mentioned above, the goal of this work is to (i) synthesize Cu_2O@TiO_2 nanocomposites by solid-state reaction, which may perform as a photocatalyst for removal of AR8 dye under UV irradiation; (ii) study the influence of adding various oxidants like H_2O_2, $Na_2S_2O_8$ and $NaIO_4$ suspended systems for improving the photocatalytic activity; and (iii) investigate the quantum yield and electrical energy per order with addition of various oxidants.

2. Materials and methods

2.1. Materials

TiO_2 (Degussa P25) was supplied from Degussa Cooperation, Germany. $CuCl_2.2H_2O$, NaOH and glucose were purchased from Aldrich chemicals, Germany. Acid Red 8 (AR8) (anionic dye) with molecular formula $C_{18}H_{14}N_2Na_2O_7S_2$, molecular weight of 480.42 g/mol, and λ_{max} 508 nm was purchased from Fluka, Germany. All oxidants such as sodium periodate ($NaIO_4$), hydrogen peroxide (H_2O_2, 30% w/v), and sodium persulphate ($Na_2S_2O_8$) were obtained from Fisher Scientific, Germany.

2.2. Synthesis of Cu_2O and Cu_2O @TiO_2

Nano Cu_2O was fabricated by co-precipitation method. Cu_2O @TiO_2 nanocomposite was prepared by two steps; one by synthesis of Cu_2O nanoparticles, followed by adding it (10 wt.% of Cu_2O) to Degussa P-25 (90 wt.% of TiO_2) for synthesis of Cu_2O @TiO_2 by solid state reaction. The powders have been mixed uniformly and formed fine powder by grinding 2 h. The resultant powders have been calcined at 500 °C for 3 h in a muffle furnace. The overall procedure for synthesis of nanocomposite is presented in Fig. 1.

2.3. Physicochemical characterization

The physicochemical properties of the synthesized Cu_2O @TiO_2 nanocomposite was observed by scanning electron microscope (SEM, JEOL, Model JSM-6360 LA, Japan) [Prior to the investigation, the samples were coated with gold using sputtering coater (model: S 150 B, Edwards High Vacuum Ltd., England)], and joint it with Energy Dispersive X-ray (EDX), X–ray diffraction (XRD, Bruker, D8 ADVACE, Germany) [Cu(Kα) radiations of wavelength ($\lambda = 1.5406$ A°) generated at 40 Kv, 40 mA], and Fourier Transform Infrared spectrophotometer (FTIR, Shimadzu-8400, Japan) [IR spectra were taken from the test samples, pressed into KBr-supported discs and scanned in the wavelength range from 400 to 4000 cm^{-1}.

2.4. Evaluation of the photocatalytic activity

The photocatalytic performance of the prepared Cu_2O@TiO_2 nanocomposite was used to evaluate the removal efficiency of AR8 dye in an aqueous solution using batch slurry photoreactor. The contents (TiO_2/dye, Cu_2O/dye, Cu_2O@TiO_2/ dye and Cu_2O@TiO_2/dye/oxidant) of the glass container were agitated by a magnetic stirrer and kept purged with air (rate 3000 ml min^{-1}). The dye solution was agitated with photocat-

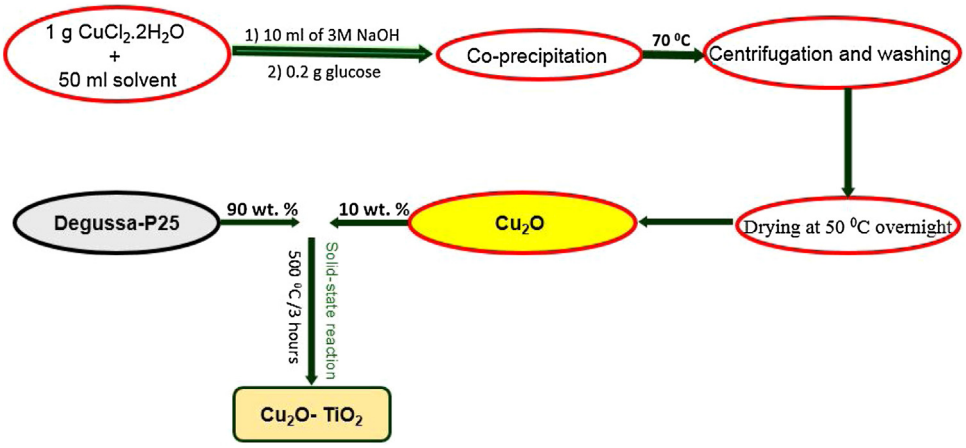

Fig. 1 – Schematic diagram for synthesis of $Cu_2O@TiO_2$ nanocomposites.

alyst for adsorption at 30 min before irradiation with UV to obtain equilibrium adsorption.

Irradiation was done with a tubular low-pressure mercury lamp with power 43 W and wavelength 254 nm (Voltarc Tubes Inc., USA). The total intensity reaching the solution was estimated 4 mWcm^{-2}. The color disappearing of AR8 dye was analyzed spectrophotometrically at its maximum absorption wavelength of 508 nm, using Shimadzu model 1601 PC double beam spectrophotometer, Japan. Samples containing $Cu_2O@TiO_2$ were taken periodically from the photoreactor and measured after filtration using 0.2 μm polyethersulfone membrane. The efficiency of the photocatalytic activity can be estimated in Eq. (1).

$$\%\text{Degradation} = [\text{Co}-\text{C}]/\text{Co} \times 100\% = [\text{Ao}-\text{A}]/\text{Ao} \times 100\% \quad (1)$$

Where Co = initial concentration of dye solution (mg/L), C = concentration of dye solution after photoirradiation (mg/L) at time t (minute). Ao is the value of absorbance of dye aqueous solution after adsorption in the dark, and A is the value of absorbance of dye aqueous solution after reaction.

3. Results and discussion

3.1. *Formation pathway of $Cu_2O@TiO_2$ nanocomposite*

In this work, $Cu_2O@TiO_2$ nanocomposite was prepared by two steps. Cu_2O nanoparticles were firstly prepared using co-precipitation method, and then Cu_2O nanoparticles were deposited on the inside and outside surface of TiO_2 by solid-state reaction, yielding the $Cu_2O@TiO_2$ nanocomposite (Fig. 1).

Firstly, Cu^{2+} ions and solvent were firstly mixed to form blue solution. Then, the addition of NaOH and glucose that supports the reduction of Cu^{2+} to Cu^{+} ions. The addition of glucose during the synthesis of Cu_2O associates to reduce the rate of agglomeration and also improve the homogeneity and the distribution of this particles with small grain size [23]. After increase the temperature from room temperature to 70 °C, a large number of Cu_2O were formed at short time. Secondly, Cu_2O was added to Degussa P-25, the ions of Cu^{+} may be diffused and adsorbed on the surface of TiO_2 as well as absorbed into the interstitial space in TiO_2 at high calcination temperature, yielding $Cu_2O@TiO_2$ nanocomposite because TiO_2 is used as a substrate with associated of low amount of Cu_2O (10 wt.%) [19,24].

3.2. *Characterization of $Cu_2O@TiO_2$ nanocomposite*

Fig. 2 (a) shows the SEM of the prepared $Cu_2O@TiO_2$ nanocomposite with high homogeneity and uniformity of aggregated semi-spherical shape. The average diameter of grain size of 56 nm. The EDX of the prepared $Cu_2O@TiO_2$ nanocomposite stated that the existence of considerable amounts of Cu, Ti, and O which confirmed that the successful fabrication of high purity of $Cu_2O@TiO_2$ nanocomposite were noticed by the existence of the distinctive energy peaks for Ti and Cu without any impurities (Fig. 2b). The spectrum shows the strong Ti signal at about 4.5 eV and a weak signal at about 0.45 eV with atomic percentage of 39.25%. Also, a weak signal at about 0.45 eV for oxygen was detected with atomic percentage of 48.52%. The two weak signals at about 0.94 and 8.04 eV for copper were detected with atomic percentage of 12.23%.

Fig. 2 (c) shows the XRD pattern of the fabricated $Cu_2O@TiO_2$ nanocomposite which displays the diffraction peaks at $2\theta = 25.23, 27.31, 35.42, 36.02, 37.82, 38.66, 47.97, 48.73, 54.04, 55.05$ and 62.61, which match to anatase and rutile titania (JCPDS card No 021-1272 and 021–1276), respectively and also pure cubic Cu_2O (JCPDS 99-0041) [25,26]. Compared to Degussa P-25 TiO_2, $Cu_2O@TiO_2$ nanocomposite has three additional XRD peaks that located at 36.02, 62.61, and 73.54 which fits to the (111), (220) and (311) and ascribed to cuprite phase as well as stated that Cu_2O are really found on to the surface of the P25 TiO_2 [16]. It is indicated that the combination of Cu_2O in the crystal structure of TiO_2 which has not any effect on the structure of Degussa P-25 and this structure is preserved. These findings are demonstrated that a two-phase composition of TiO_2 and Cu_2O exist in the $Cu_2O@TiO_2$ heterostructure.

The FTIR spectrum of $Cu_2O@TiO_2$ nanocomposite (Fig. 2d) shows a band at 3471 cm^{-1}, which is distinctive of the non-hydrogen bonded surface hydroxyl groups. Also, the peak observed at 1638 cm^{1} is ascribed to the bending mode of the adsorbed water [27]. The characteristic vibration band of the

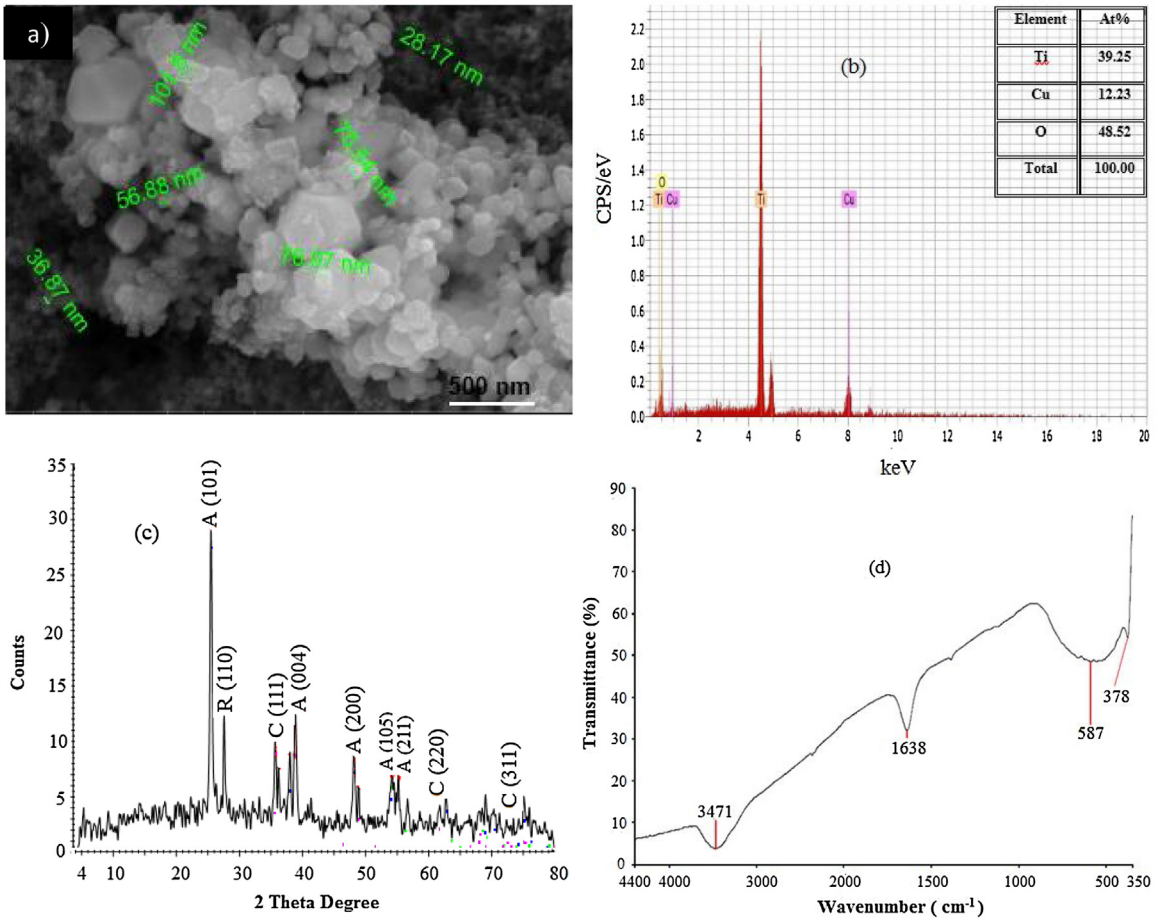

Fig. 2 – (a) SEM, (b) EDX, (c) XRD, and (d) FT-IR of $Cu_2O@TiO_2$ nanocomposite. [A: anatase, R: rutile, and C: cuprite].

inorganic Cu—O has been detected at 378 cm^{-1} whereas the representative band of the inorganic Ti—O has been observed at 587 cm^{-1} [16].

3.3. *Photocatalysis of acid red 8 dye*

3.3.1. *Degradation kinetics*

The decomposition kinetics of AR8 dye by TiO_2, Cu_2O, and its composite $Cu_2O@TiO_2$ were assessed by following the Langmuir-Hinshelwood model [11]. When the chemical concentration Co is millimolar solution the integrated form of Eq. (2) be an apparent first order equation.

$$\ln(C_o/C) = k_{app}t \quad (2)$$

Where, k_{app} represents the apparent first order rate constant, C_o and C are concentration before and photocatalytic reaction, respectively. The half-life time ($t^{0.5}$) of the first order reaction is the time required for the reactants to be degraded to the half of their C_o. The relationship between $t^{0.5}$ and k_{app} is given by Eq. (3).

$$t^{0.5} = 0.693/k_{app} \quad (3)$$

3.3.2. *Comparison between TiO_2, Cu_2O and its composite $Cu_2O@TiO_2$*

The decomposition of AR8 dye as an organic contaminant model has been achieved by photocatalytic performance using TiO_2 P-25, Cu_2O and it surface modified $Cu_2O@TiO_2$ nanocomposite as photocatalysts at room temperature. The destruction of AR8 dye was assessed by reducing the C_o at λ_{max} 508 nm due to the azo bond (N=N). The AR8 dye was completely degraded at around 90 min with obeyed the pseudo-first-order kinetic models (Figure not shown). In Table 1, the decomposition rate follows the order $Cu_2O@TiO_2 > Cu_2O > TiO_2$. The rate of removal by pure Cu_2O was higher than that of pure TiO_2 which may be due to the low band gap of Cu_2O. The most effective catalytic system is obtained by using combined $Cu_2O@TiO_2$ system which can be ascribed to the more efficient separation of photoinduced electron-hole (e^-/h^+) pairs, and also improve the surface-active sites in composite [17,20,29].

3.3.3. *Influence of various oxidation processes on the degradation by addition of electron acceptors*

One of the significant drawbacks of the photocatalysis is the electron-hole recombination which signifies the major energy-wasting step and subsequently leads to the reduction of the quantum yield. So, the deferring of electron-hole recombination by addition of irreversible electron acceptors in

Table 1 – Collective data of apparent rate constants, half-life times, and reaction orders for degradation of AR8 dye [conc. of catalyst 0.1 g/l].

Catalytic system	Concentration of oxidant (M)	k_{app} (min^{-1})	$t^{0.5}$ (min)	Apparent reaction order (n)
UV/Cu_2O	–	124×10^{-4}	5.6	–
UV/TiO_2		84.0×10^{-4}	8.3	
UV/Cu_2O@TiO_2		150×10^{-4}	4.6	
UV/Cu_2O@TiO_2/H_2O_2	2×10^{-3}	182×10^{-4}	3.8	0.4
	4×10^{-3}	278×10^{-4}	2.5	
	12×10^{-3}	375×10^{-4}	1.8	
	14×10^{-2}	531×10^{-4}	1.3	
	28×10^{-2}	1257×10^{-4}	0.6	
	45×10^{-2}	1834×10^{-4}	0.4	
UV/Cu_2O@TiO_2/$S_2O_8^{2-}$	1×10^{-3}	302×10^{-4}	2.3	1.2
	2×10^{-3}	455×10^{-4}	1.5	
	4×10^{-3}	983×10^{-4}	0.7	
UO	8×10^{-3}	3651×10^{-4}	0.2	1.2
UV/Cu_2O@TiO_2/IO_4^-	4.0×10^{-5}	1297×10^{-4}	0.50	0.2
	7.4×10^{-4}	2001×10^{-4}	0.30	
	1.0×10^{-3}	2846×10^{-4}	0.20	
	21×10^{-3}	3664×10^{-4}	0.18	
	48×10^{-3}	4881×10^{-4}	0.14	
	11×10^{-2}	7229×10^{-4}	0.10	

order to increase the rate of photocatalysis, especially in high concentration of toxic dyes. The observed drastically accelerated the decomposition were attributed to the improving the electron scavenging from the added inorganic oxidants. The merits of addition of electron acceptors is to avoid the recombination via (i) increase the number of trapped electrons; (ii) generation of more radicals and other oxidizing species ; (iii) increasing the oxidation rate of the intermediate compounds and (iv) avoiding the problems of low oxygen concentration [28–30]. Hence, various concentrations of oxidants (H_2O_2, $Na_2S_2O_8$ and $NaIO_4$) were added to the AR8 dye solution in the presence of the combined Cu_2O@TiO_2 system that illustrated in Fig. 3. The introduction of inorganic oxidants is utilized for enhancing the rate of degradation of AR8 dye through better scavenge the ejected electrons of TiO_2 and hence the survival time h^+ at Cu_2O will be higher and subsequently reacts effectively with AR8 dye. The effect of the concentration of various oxidants is described well as follow;

(a) H_2O_2

The UV/Cu_2O@TiO_2/H_2O_2 system is used to trap the electrons at conduction band and formation of more $^{\bullet}OH$ radicals from generation for superoxide anion radicals ($^{\bullet}O_2^-$) and homolytic cleavage of bonds of two hydroxyl groups during the photolysis, which enhancing the rate of photocatalytic reaction. H_2O_2 is used as an electron acceptor than oxygen in other mechanisms and subsequently the rate of recombination will decrease [11]. Also, H_2O_2 is more electropositive than O_2 that result from two hydrogen atoms bonded to oxygen atoms (H—O—O—H).

To deep the illustration of into the effective reactivity of H_2O_2/ Cu_2O@TiO_2 system on the decomposition of AR8 dye was studied at various concentration of H_2O_2 in Fig. 3 (a). It has been stated that the enhanced photo-destruction rate with increasing the dose of H_2O_2. Also, the k_{app} was increased from 182×10^{-4} to 1834×10^{-4} min^{-1} when the concentration of H_2O_2 was ranged from 2×10^{-3} to 45×10^{-2} M (Table 1). The effect of rate determining species is expressed by a power law relation

$$k_{app} = K[H_2O_2]^n \quad (4)$$

Where k_{app} and K are the apparent and the true rate constants, respectively. The n is the order of the photocatalytic reaction. From Fig. 3(b), the value of n was 0.4 (Table 1). The rate of AR8 dye degradation using UV/Cu_2O@TiO_2/H_2O_2 system is better when compared to UV/Cu_2O@TiO_2 alone. This may be ascribed to (i) trap of the photogenerated conduction band electrons of Cu_2O@TiO_2 by H_2O_2, which is more efficient than trapping by O_2, according to the following reaction [31].

$$H_2O_2 + e^-_{(cb)} \rightarrow {}^-OH + {}^{\bullet}OH \quad (5)$$

(ii) generate other oxidizing species ($^{\bullet}OH$), which can contribute to the oxidative decay process; and (iii) after illumination, substantial photolysis of the H_2O_2 would produce more hydroxyl radicals (Eq. 6) [32].

$$H_2O_2 + h\nu \rightarrow 2{}^{\bullet}OH \quad (6)$$

In summary, the increasing the H_2O_2 concentrations leads to an increase in both electron scavenging action, and hydroxyl radicals, which oxidize the dye and lead to a higher rate of decomposition.

(b) Peroxydisulphate ions $S_2O_8^{2-}$

Fig. 3(c) displays the influence of adding $S_2O_8^{2-}$ to combined Cu_2O@TiO_2 system on the destruction of AR8 dye. It was found that the rate of removal was enhanced with the addition of a low concentration of the $S_2O_8^{2-}$ (1×10^{-3} M) to UV/Cu_2O@TiO_2 system. According to a first-order model for dye destruction, it has been found that the enhanced photodegradation rate is result from the increasing the concentration of $S_2O_8^{2-}$. Also, the k_{app} was increased from 302×10^{-4} to 3651×10^{-4} min^{-1} when the concentration of

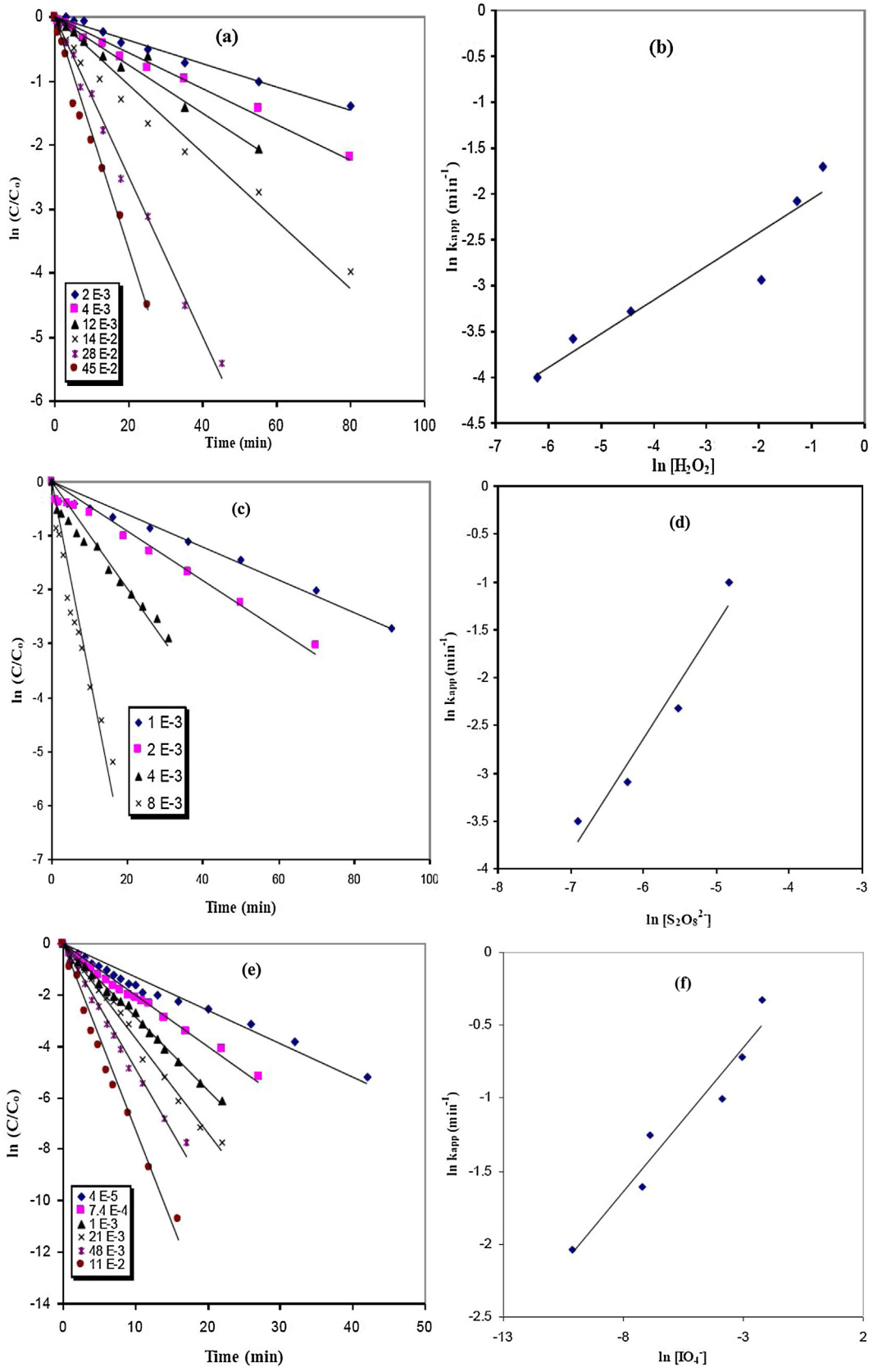

Fig. 3 – (a, c, e) Change of ln (C/C_o) with time at different concentrations of H_2O_2, $S_2O_8^{2-}$, and IO_4^-, respectively, and (b, d, f) Change of ln k_{app} (min^{-1}) with ln [H_2O_2], ln [$S_2O_8^{2-}$], and ln [IO_4^-], respectively.

Table 2 – Collective data of apparent rate constants, electrical energy per order and apparent quantum yield for degradation of acid red 8 dye [conc. of catalyst 0.1 g/l].

Catalytic system	Concentration of oxidant (M)	k_{app} (min^{-1})	E_{EO} (kWh/m^3)	Q_{app} % (mol/Einstein)
UV/Cu_2O	–	124×10^{-4}	526.3	1.07
UV/TiO_2		84.0×10^{-4}	769.2	0.73
UV/Cu_2O@TiO_2		150×10^{-4}	333.3	1.3
UV/Cu_2O@TiO_2/H_2O_2	2×10^{-3}	182×10^{-4}	357.1	1.58
	4×10^{-3}	278×10^{-4}	238.1	2.41
	12×10^{-3}	375×10^{-4}	175.4	3.25
	14×10^{-2}	531×10^{-4}	125	4.60
	28×10^{-2}	1257×10^{-4}	52.6	11.0
	45×10^{-2}	1834×10^{-4}	36	16.0
UV/Cu_2O@TiO_2/$S_2O_8^{2-}$	1×10^{-3}	302×10^{-4}	217.4	2.62
	2×10^{-3}	455×10^{-4}	145	4.0
	4×10^{-3}	983×10^{-4}	67.1	8.52
UV/CuO@TiO/SO	8×10^{-3}	3651×10^{-4}	18.1	31.6
UV/Cu_2O@TiO_2/IO_4^-	4.0×10^{-6}	1297×10^{-4}	51	11.2
	7.4×10^{-4}	2001×10^{-4}	33	17.3
	1.0×10^{-3}	2846×10^{-4}	23.2	24.7
	21×10^{-3}	3664×10^{-4}	18.1	31.8
	48×10^{-3}	4881×10^{-4}	13.5	42.3
	11×10^{-2}	7229×10^{-4}	9.1	62.7

$S_2O_8^{2-}$ was ranged from 1×10^{-3} to 8×10^{-3} M (Table 1). The complete decomposition of the dye in a short time (20 min) at conc. 8×10^{-3} M of $S_2O_8^{2-}$. The rate order of photocatalytic reaction with respect to $S_2O_8^{2-}$, which was obtained from Fig. 3(d), was found to be 1.2 (Table 1).

The addition of $S_2O_8^{2-}$ ions could have increased the photocatalytic performance due to the interaction with light and its interaction with Cu_2O@TiO_2. The photolysis of persulfate leads to the formation of sulphate radicals whose redox potential 2.5–3.1 V/NHE is higher than that of $S_2O_8^{2-}$ ions (1.96 V/NHE) [32]. The $S_2O_8^{2-}$ anions can trap the electrons that formed from the conduction band of Cu_2O@TiO_2 more than the electrons from O_2, and thus formed other oxidant $SO_4^{\bullet-}$ (Eq. 7) [33]

$$S_2O_8^{2-} + e^-_{(cb)} \rightarrow SO_4^{2-} + SO_4^{\bullet-} \quad (7)$$

Upon irradiation, the $SO_4^{\bullet-}$ is also generated and can contribute in the photocatalytic reaction with water for formation of $^{\bullet}OH$, according to Eqs. (8 and 9).

$$S_2O_8^{2-} + h\nu \rightarrow 2SO_4^{\bullet-} \quad (8)$$

$$SO_4^{\bullet-} + H_2O \rightarrow {}^{\bullet}OH + SO_4^{2-} + H^+ \quad (9)$$

So, the increased concentrations of the $S_2O_8^{2-}$ have increased the trapping of the electrons from the conduction bands of Cu_2O@TiO_2 and the production of $SO_4^{\bullet-}$ and $^{\bullet}OH$. These two factors are responsible for higher rate of photodecomposition of AR8 dye.

(c) Periodate ion IO_4^-

Oxyhalogens have atom of oxygen and another atom of halogen as a central atom. The difference in polarization between oxygen and halogen leads to the capturing the ejected electron. The effect of oxyhalogen system is extremely based on the differences in the electronegativity and the atomic radius of the halogen [34]. The electropositive halogen oxidant is used as a stronger electron scavenger via the generation of h_{VB}^+ and formation of $^{\bullet}OH$.

The increasing of the atomic radius leads to the decreasing of the electronegativity that result from capturing the ejected electron by halogen. Hence, the atomic radius of I has higher than that of Cl or Br and it has more bonded with oxygen than Cl or Br, and the ability of electrons over photocatalyst will be higher. So, the UV/Cu_2O@TiO_2/ $IO_4^{\bullet}$ is the best system for decomposition of AR8 dye by the oxyhalogen oxidant.

Fig. 3(e) shows the influence of addition of various concentration of periodate ions to UV/Cu_2O@TiO_2 system on the destruction of AR8 dye. The addition of very low concentrations of IO_4^- (4.0×10^{-5} M) to Cu_2O@TiO_2 has resulted in a higher decomposition rate than UV/Cu_2O@TiO_2 only. Also, when increasing the concentration of the periodate to (11×10^{-2} M) has resulted in dye destruction after the shortest time (18 min). According to the IO_4^-, The reaction rate order is 0.2 (Fig. 3(f) and Table 1). The scavenging of the electrons by Cu_2O@TiO_2/IO_4^- system leads to the improvement of the photocatalytic decomposition of AR8 dye, which is more efficient than trapping with O_2 or $S_2O_8^{2-}$ as follows [35];

$$IO_4^- + 8e^-_{(cb)} + 8H^+ \rightarrow 4H_2O + I^- \quad (10)$$

Also, upon irradiation, the photolytic decomposition of the IO_4^-, involves the formation of a number of highly reactive radical- and non-radical intermediates ($IO_3^{\bullet}$, $^{\bullet}OH$, $O^{\bullet-}$ and $IO_4^{\bullet}$) (Eqs. 11–13) as follows [35].

$$IO_4^- + h\nu \rightarrow IO_3^{\bullet} + O^{\bullet-} \quad (11)$$

$$O^{\bullet-} + H^+ \leftrightarrow {}^{\bullet}OH \quad (12)$$

$$^{\bullet}OH + IO_4^- \rightarrow OH^- + IO_4^{\bullet} \quad (13)$$

These intermediates are responsible for the enhancing the decomposition of organic compounds [32]. Increasing the con-

centration of IO_4^-, the number of available h^+_{VB} is increased and their long lifetime would be beneficial for the decomposition of AR8 dye (Fig. 3e). This is may be due to the trapping of the electrons in conduction bands of combined $Cu_2O@TiO_2$ system and also the production of highly reactive oxygen species such as IO_3^-, $O^{\bullet -}$, O_3, $^{\bullet}OH$ and $IO_4^{\bullet}$. This led to a higher rate of degradation [32,35].

3.3.4. *Quantum efficiency of photocatalytic reaction*

The quantification of heterogenous catalysis can be determined by the estimation of quantum yield, which may be defined as the rate at which reactant molecules disappear or product molecules are formed, divided by the number of photons absorbed per unit time. With dispersed catalysts, a large fraction of the incident light is either reflected or scattered and not absorbed by the dye solution. There does not usually exist any possibility to determine experimentally the amount of light absorbed by the photocatalyst. In order to bypass the difficulty of determining quantum yields in heterogeneous photocatalysis, another parameter often reported is the apparent quantum yield (Q_{app}) which defined as shown in Eq. (14) [36,37]

$$\text{Apparentquantumyield}(Q_{app}, \text{mol/Einstein}) = \text{Rateof disappearanceofreactantmolecules/Rateofincident photonsinsidereactorcell} = k_{app}\, C_o/I \quad (14)$$

Where k_{app} is the apparent first-order rate constant, C_o is the initial dye concentration and I is the total intensity of incident photons entering the reactor cell. It was observed from Table 2 that Q_{app} for UV/$Cu_2O@TiO_2/IO_4$-system is higher than those for UV/$Cu_2O@TiO_2/H_2O_2$ and UV/$Cu_2O@TiO_2/S_2O_8^{2-}$ systems. This may be due to the higher activity of periodate when compared to hydrogen peroxide and persulfate as obtained in the previous studies [33,36].

3.3.5. *Figure of merit*

Nowadays, the economic study of each process is a significant factor which it includes the major fraction of operating cost. Hence, it is necessary to study the electrical energy consumption of the AOPs under experimental conditions. The electrical energy per order (E_{EO}) is an informative factor for the photocatalytic degradation because it obeys the first order kinetic model [6]. The figures of merit E_{EO} allows for a rapid determination of the electrical energy cost and they indicate the total power required. For comparative purpose, the treatment efficiencies for the different processes are evaluated through the E_{EO} values. The E_{EO} is defined as the number of kWh of electrical energy required to reduce the concentration of pollutant by one order of magnitude (90%) in 1 m^3 of contaminated water. Considering first-order degradation kinetics, the UV doses were calculated for all AOPS using Eq. (15) [38]. From the UV doses, the simplest form of the estimation of E_{EO} can also be calculated using Eq. (16) [37].

$$\text{UVDose} = [\text{Lamppower(kW)} \times \text{Time(h)} \times 1000] / [\textit{Treatedvolume(L)}] \quad (15)$$

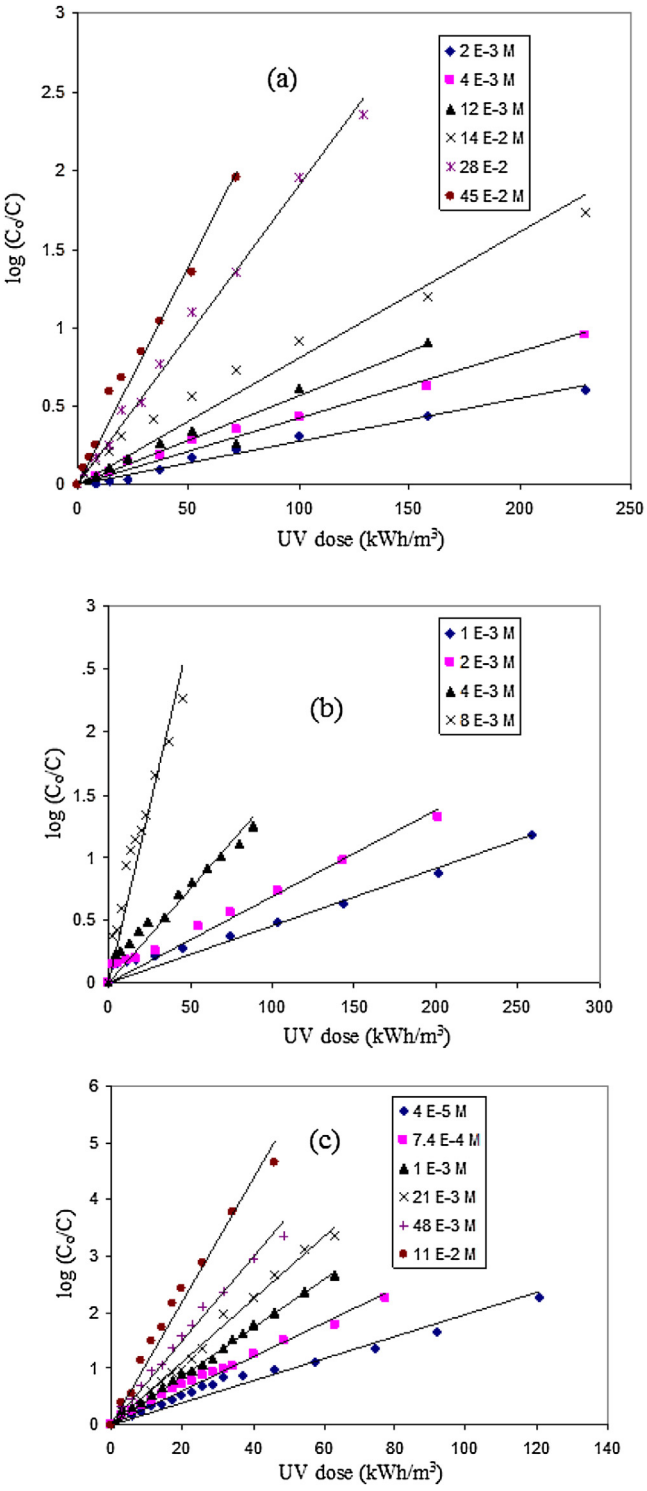

Fig. 4 – Change of log (Co/C) with UV dose for degradation of AR8 dye using 0.1 gm of $Cu_2O@TiO_2$ with different concentrations of (a) H_2O_2, (b) $S_2O_8^{2-}$, and (c) IO_4^-, respectively.

$$E_{EO} = UVDose/[Log(C_o/C)] \quad (16)$$

From Eq. (16), the E_{EO} values were obtained from the inverse of the slope of a plot of log (C_o/C) versus UV dose (Fig. 4). It was found that the figure-of-merit E_{EO} is appropriate for estimating the electrical energy efficiency. It is not only proving the reduction in the needed electricity by the photocatalytic system, but also offering the considerable influence of the UV dose on the E_{EO} in the process. The E_{EO} values were found to be dependent on the concentration of H_2O_2, $S_2O_8^{2-}$, and IO_4-. Also, the E_{EO} values of additional oxidants to UV/Cu_2O@TiO_2 system is lower than that blank UV/Cu_2O@TiO_2 system which indicate that the lower energy consumption is due to the greater applied potential and generation of highly reactive radical species at the higher potential. The E_{EO} values show that the addition of periodate exhibited also a low energy consumption compared to peroxide and persulfate (Table 2). In summary, these findings can be applied for designing photocatalytic system with less consumption of electrical energy, higher rate constant and lower operation cost.

3.3.6. *Comparison between various oxidants*

This study has presented that the three oxidants, peroxide, persulfate and periodate, have enhanced the rate of UV-induced decomposition of AR8 dye in the presence of combined Cu_2O@TiO_2 system. This enhancement is as a result of the scavenging the active species radicals, such as hydroxyl radicals, and holes by the inorganic ions [29]. It can be seen that the addition of very low concentrations IO_4^- to Cu_2O@TiO_2 has resulted in a higher decomposition rate than UV/Cu_2O@TiO_2, UV/Cu_2O@TiO_2/H_2O_2 and UV/Cu_2O@TiO_2/$S_2O_8^{2-}$, thus indicating the effectiveness of IO_4^- over H_2O_2 and $S_2O_8^{2-}$ as a result of higher of k_{app}, shorter $t^{0.5}$, higher Q_{app}, and lower E_{EO}. The highly reactive radical species in periodate may directly abstract H from AR8 dye molecules. So, the irradiated IO_4^- solution can quickly oxidize the AR8 molecules [39].

4. Conclusions

In summary, we revealed that the facile and proficient approach for the fabrication of Cu_2O@TiO_2 nanocomposite via a solid-state approach. The formation of this composite was revealed by SEM-EDX, XRD and FT-IR. The combined Cu_2O@TiO_2 heterojunction system exhibited much higher photocatalytic activity than that of pristine Cu_2O and TiO_2. This is due to the transfer of electrons from Cu_2O to the conduction band of TiO_2 is concurrently with the photogenerated holes at the valence band of Cu_2O, which facilitates the electron and hole separation and improves the photocatalytic activity of Cu_2O@TiO_2 heterojunction nanocomposite. It was found that the heterogeneous photocatalytic degradation, under UV illumination, using the following order: Cu_2O@TiO_2/ $NaIO_4$ > Cu_2O@TiO_2/$Na_2S_2O_8$ > Cu_2O@TiO_2/H_2O_2 > Cu_2O > TiO_2. The photocatalytic activity enhancement was attributed to the various reactive oxygen species like $^{\bullet}OH$ and $IO_4^{\bullet}$. The higher decolorization and quantum efficiency and lower energy per order and energy consumption of combined Cu_2O@TiO_2 system with oxidants than bare Cu_2O@TiO_2. The combination of Cu_2O@TiO_2 nanocomposite with various oxidants may bring a new insight into highly efficient photocatalytic applications in the future.

Conflicts of interest

The authors declare no conflicts of interest.

REFERENCES

[1] Li Y, Wang P, Huang C, Yao W, Wu Q, Xu Q. Synthesis and photocatalytic activity of ultrafine Ag_3PO_4 nanoparticles on oxygen vacated TiO_2. Appl Catal B Environ 2017;205:489–97.

[2] Luo Y, Huang J. Hierarchical-structured anatase-titania/cellulose composite sheet with high photocatalytic performance and antibacterial activity. Chem Eur J 2015;21:2568–75.

[3] Oturan MA, Aaron JJ. Advanced oxidation processes in water/wastewater treatment: principles and applications. A review. Crit Rev Environ Sci Technol 2014;44:2577–641.

[4] Shalaby T, Hamad H, Ibrahim E, Mahmoud O, Al-Oufy A. Electrospun nanofibers hybrid composites membranes for highly efficient antibacterial activity. Ecotoxicol Environ Safe 2018;162:354–64.

[5] Lau Y-Y, Wong Y-S, Teng T-T, Morad N, Rafatullah M, Ong S-A. Coagulation-flocculation of azo dye Acid Orange 7 with green refined laterite soil. Chem Eng J 2014;246:383–90.

[6] Hamad H, Bassyouni D, El-Ashtoukhy E, Amin N, El-Latif MA. Electrocatalytic degradation and minimization of specific energy consumption of synthetic azo dye from wastewater by anodic oxidation process with an emphasis on enhancing economic efficiency and reaction mechanism. Ecotoxicol Environ Safe 2018;148:501–12.

[7] El-Ashtoukhy E-SZ, Amin NK, El-Latif MMA, Bassyouni DG, Hamad HA. New insights into the anodic oxidation and electrocoagulation using a self gas stirred reactor: a comparative study for synthetic C.I Reactive Violet 2 wastewater. J Clean Prod 2017;167:432–46.

[8] Yang K, Yu J, Guo Q, Wang C, Yang M, Zhang Y, et al. Comparison of micropollutants' removal performance between pre-ozonation and post-ozonation using a pilot study. Water Res 2017;111:147–53.

[9] Cui Y, Liu X-Y, Chung T-S, Weber M, Staudt C, Maletzko C. Removal of organic micro-pollutants (phenol, aniline and nitrobenzene) via forward osmosis (FO) process: evaluation of FO as an alternative method to reverse osmosis (RO). Water Res 2016;91:104–14.

[10] Elkady M, Shokry H, Hamad H. Microwave-assisted synthesis of magnetic hydroxyapatite for removal of heavy metals from groundwater. Chem Eng Technol 2018;41:553–62.

[11] Hamad H, Bailón-García E, Maldonado-Hódar FJ, Pérez-Cadenas AF, Carrasco-Marín F, Morales-Torres S. Synthesis of Ti_xO_y nanocrystals in mild synthesis conditions for the degradation of pollutants under solar light. Appl Catal B Environ 2019;241:385–92.

[12] Hamad HA, Sadik WA, Abd El-latif MM, Kashyout AB, Feteha MY. Photocatalytic parameters and kinetic study for degradation of dichlorophenol-indophenol (DCPIP) dye using highly active mesoporous TiO_2 nanoparticles. J Environ Sci 2016;43:26–39.

[13] Fujishima A, Rao TN, Tryk DA. Titanium dioxide photocatalysis. J Photochem Photobiol C: Photochem Rev 2000;1:1–21.

[14] Kim H, Yoo H-Y, Hong S, Lee S, Lee S, Park B-S, et al. Effects of inorganic oxidants on kinetics and mechanisms of WO_3-mediated photocatalytic degradation. Appl Catal B Environ 2015;162:515–23.
[15] Hamad H, Abd El-latif M, Kashyout A, Sadik W, Feteha M. Synthesis and characterization of core–shell–shell magnetic ($CoFe_2O_4$–SiO_2–TiO_2) nanocomposites and TiO_2nanoparticles for the evaluation of photocatalytic activity under UV and visible irradiation. New J Chem 2015;39:3116–28.
[16] Kaviyarasan K, Vinoth V, Sivasankar TH, Asiri AM, Wu JJ, Anandan S. Photocatalytic and photoelectrocatalytic performance of sonochemically synthesized Cu_2O@TiO_2 heterojunction nanocomposites. Ultrason Sonochem 2019;51:223–9.
[17] Jin Q, Fujishima M, Iwaszuk A, Nolan M, Tada H. Loading effect in copper (II) oxide cluster-surface-modified titanium (IV) oxide on visible-and UV-light activities. J Phys Chem C 2013;117:23848–57.
[18] Fei X, Li F, Cao L, Jia G, Zhang M. Adsorption and photocatalytic performance of cuprous oxide/titania composite in the degradation of acid red B. Mater Sci Semicond Process 2015;33:9–15.
[19] Ch-Y Kuo, Ch-H Wu, Lina H-Y. Synergistic effects of TiO_2 and Cu_2O in UV/TiO_2/zeolite-based systems on photodegradation of bisphenol A. Environ Technol 2014;15:1851–7.
[20] Hu Z, Wang X, Dong H, Sh Li, Li X, Li L. Efficient photocatalytic degradation of tetra bromodiphenyl ethers and simultaneous hydrogen production by TiO_2-Cu_2O composite films in N_2 atmosphere: influencing factors, kinetics and mechanism. J Hazard Mater 2017;340: 1–15.
[21] Yin H, Wang X, Wang L, Nie Q, Zhang YY, Wu W. Cu_2O/TiO_2 heterostructured hollow sphere with enhanced visible light photocatalytic activity. Mater Res Bull 2015;72:176–83.
[22] Ajmal A, Majeed I, Malik RN, Iqbal M, Nadeem MA, Hussain I, et al. Photocatalytic degradation of textile dyes on Cu_2O-CuO/TiO_2 anatase powders. J Environ Chem Eng 2016;4:2138–46.
[23] Luevano-Hipolito E, Torres-Martınez LM, Sanchez-Martınez D, Cruz MRA. Cu_2O precipitation-assisted with ultrasound and microwave radiation for photocatalytic hydrogen production. Int J Hydrog Energy 2017;42:12997–3010.
[24] Wang Y, Tao J, Wang X, Wang Z, Zhang M, He G, et al. A unique Cu_2O/TiO_2 nanocomposite with enhanced photocatalytic performance under visible light irradiation. Ceram Int 2017;43:4866–72.
[25] Hamad H, El-latif MA, Kashyout A, Sadik W, Feteha M. Optimizing the preparation parameters of mesoporous nanocrystalline titania and its photocatalytic activity in water: physical properties and growth mechanisms. Process Saf Environ Prot 2015;98:390–8.
[26] Wang X, Dong H, Hu Z, Qi Z, Li L. Fabrication of a Cu_2O/Au/TiO_2 composite film for efficient photocatalytic hydrogen production from aqueous solution of methanol and glucose. Mater Sci Eng B 2017;219:10–9.
[27] Hamad H, Bailón-García E, Morales-Torres S, Pérez-Cadenas AF, Carrasco-Marín F, Maldonado-Hódar FJ. Physicochemical properties of new cellulose-TiO_2 composites for the removal of water pollutants: developing specific interactions and performances by cellulose functionalization. J Environ Chem Eng 2018;6:5032–41.
[28] Yang L, Li Z, Jiang H, Jiang W, Su R, Luo SH, et al. Photoelectrocatalytic oxidation of bisphenol A over mesh of TiO_2/graphene/Cu_2O. Appl Catal B Environ 2016;183:75–85.
[29] Saleh R, Taufik A, Prakoso SP. Fabrication of Ag_2O/TiO_2 composites on nanographene platelets for the removal of organic pollutants: influence of oxidants and inorganic anions. Appl Surf Sci 2019;480:697–708.
[30] Bekkouche S, Merouani S, Hamdaoui O, Bouhelassa M. Efficient photocatalytic degradation of Safranin O by integrating solar-UV/TiO_2/persulfate treatment: implication of sulfate radical in the oxidation process and effect of various water matrix components. J Photochem Photobiol A: Chem 2017;345:80–91.
[31] Dougna AA, Gombert B, Kodom T, Djaneye-Boundjou G, Boukari SOB, Leitner NKV, et al. Photocatalytic removal of phenol using titanium dioxide deposited on different substrates: effect of inorganic oxidants. J Photochem Photobiol A: Chem 2015;305:67–77.
[32] Nguyen AT, Juang R-SH. Photocatalytic degradation of p-chlorophenol by hybrid H_2O_2 and TiO_2 in aqueous suspensions under UV irradiation. J Environ Manage 2015;147:271–7.
[33] Sadik WA. Effect of inorganic oxidants in photodecolourization of an azo dye. J Photochem Photobiol A: Chem 2007;191:132–7.
[34] Yun E-T, Yoo H-Y, Kim W, Kim H-E, Kang G, Lee H, et al. Visible-light-induced activation of periodate that mimics dye-sensitization of TiO_2: simultaneous decolorization of dyes and production of oxidizing radicals. Appl Catal B Environ 2017;203:475–84.
[35] Chen M, Chu W. Photo-oxidation of an endocrine disrupting chemical o chloroaniline with the assistance of TiO_2 and iodate: reaction parameters and kinetic models. Chem Eng J 2014;248:273–9.
[36] Irmak S, Kusvuran E, Erbatur O. Degradation of 4-chloro-2-methylphenol in aqueous solution by UV irradiation in the presence of titanium dioxide. Appl Catal B Environ 2004;54:85–91.
[37] Daneshvar N, Aleboyeh A, Khataee AR. The evaluation of electrical energy per order (EE/O) for photooxidative decolorization of four textile dye solutions by the kinetic model. Chemosphere 2005;59:761–7.
[38] Lam S-M, Sin J-C, Abdullah AZ, Mohamed AR. Photocatalytic degradation of resorcinol, an endocrine disrupter, by TiO_2 and ZnO suspensions. Environ Technol 2013;34:1097–106.
[39] Qamar M, Saquib M, Muneer M. Photocatalytic degradation of two selected dye derivatives, chromotrope 2B and amido black 10B, in aqueous suspensions of titanium dioxide. Dyes Pigm 2005;65:1–9.